Coupling Conditions and Two Level Methods on Graphs

Martin J. Gander, Florence Hubert, Magali Ribot

1 Introduction

We are interested in modeling channel systems governed by partial differential equations. A typical example are water channels, as shown in Figure 1 on the left, see e.g. [8, 11, 3, 5]. To model flow in such channels, one uses in general the 2D shallow water equations. For large networks, it would be advantageous to use a simpler 1D model along the channels [10], as indicated in Figure 1 going from the middle to the right. One could then simply use the 1D Saint Venant equations (1871) throughout the network,

$$\partial_t h + \partial_x (hv) = 0, \quad \partial_t (hv) + \partial_x (hv^2 + \frac{1}{2} g h^2) = -gh\partial_x b, \tag{1}$$

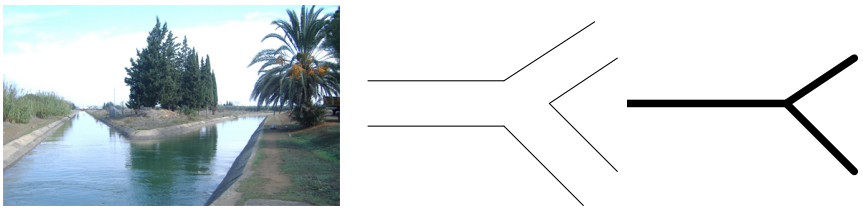

Fig. 1 Left: Irrigation channels in the vallée de la Medjerda, Tunisia. Middle: geometric shape of a junction. Right: simpler one dimensional approximation of the junction.

Martin J. Gander
Université de Genève, e-mail: martin.gander@unige.ch

Florence Hubert
Aix-Marseille University, CNRS, I2M, Marseille, France e-mail: florence.hubert@univ-amu.fr

Magali Ribot
Institut Denis Poisson,Université d'Orléans, CNRS, Université de Tours, France, e-mail: magali.ribot-barre@univ-orleans.fr

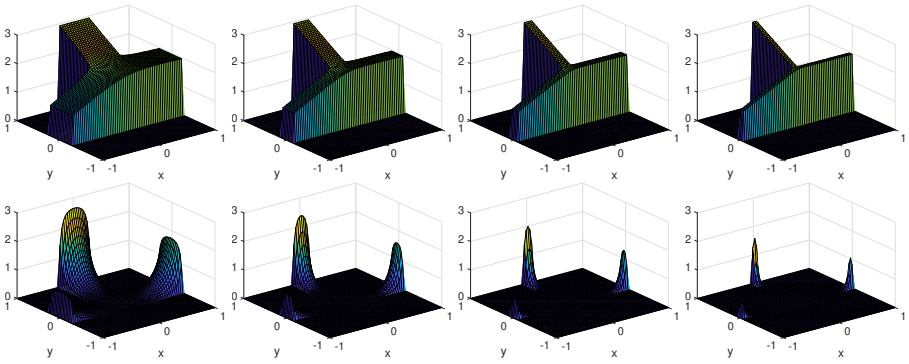

Fig. 2 Laplace problem on a junction with diminishing channel width and Dirichlet boundary conditions equal to 1, 2 and 3 at the channel ends. Top: zero Neumann conditions along the channel sides. Bottom: zero Dirichlet conditions along the channel sides.

where h is the water height, v is the velocity to be computed, b is the given topography, and g the constant of gravitation. The 1D Saint Venant equation (1) needs to be solved on each branch of the network, where x denotes the coordinate along the branch. Questions for the simplified one dimensional model for the network are then how the one dimensional model should be coupled at junctions [14, 1, 9], and also if the network is very large, for example the human blood system [13, 12], how one should solve such problems in a scalable way [4], see also [7, 2] for reviews on PDEs on networks. We start here with the simpler Laplace problem on such a network, to investigate coupling conditions and scalability of such a network solver.

2 Coupling Conditions for the Laplace Problem

We consider the Laplace problem $\Delta u = 0$ on a T-junction and start with a numerical simulation shown in Figure 2. We solve the Laplace problem first with zero Neumann boundary conditions on the channel sides, and Dirichlet boundary conditions with values 1, 2 and 3 at the channel ends, and diminish the channel width in the top row of Figure 2 from the left to the right to see what type of limit is approached by the numerical solution. We see that indeed the solution seems to approach a limit: on each branch the solution is linear along the branch, i.e. solution of the 1D Laplace problem, and coupled with a specific condition at the junction. To see the importance of Neumann conditions on the channel sides, we repeat the same experiment with zero Dirichlet boundary conditions, see the bottom row of Figure 2. Clearly, in that case, there is no flow remaining through the network, and thus the lateral boundary conditions are very important for obtaining an interesting lower dimensional limiting model.

In order to determine the coupling conditions in the lower dimensional model, we use now a domain decomposition idea, as indicated in Figure 3. We decompose the

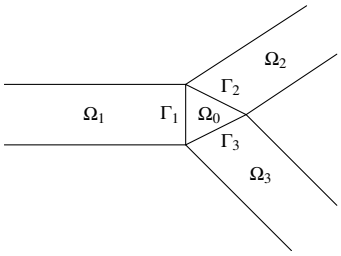

Fig. 3 Domain decomposition to obtain coupling conditions at the junction.

junction in 2D into four subdomains, three Ω_j, $j = 1, 2, 3$ representing the incoming channels, and the coupling domain Ω_0 in the middle. In order to have an equivalent Laplace problem on these four subdomains in 2D, the coupling conditions on the interfaces Γ_j, $j = 1, 2, 3$ between the subdomains must be matching Dirichlet and Neumann data,

$$u_j = u_0 \quad \text{and} \quad \partial_n u_j = \partial_n u_0, \tag{2}$$

where ∂_n denotes the unit outer normal derivative for the subdomain Ω_0. Integrating the equation on the coupling subdomain Ω_0, and using the divergence theorem, we get

$$0 = \int_{\Omega_0} \Delta u_0 = \int_{\partial\Omega_0} \partial_n u_0 = \sum_j \int_{\Gamma_j} \partial_n u_j,$$

and hence, when the channel width goes to zero equally for all channels, we get

Theorem 1 *The coupling conditions for the Laplace problem on networks at junctions in a reduced 1D model are*

$$u_j = u_0 \quad \textit{and} \quad \sum_j \partial_n u_j = 0, \tag{3}$$

where ∂_n denotes now the outgoing normal derivative along each channel direction.

These are the analog of Kirchhoff's laws for electric circuits, which he discovered being a student, and on which he then wrote his PhD thesis. This result is well known and can be found for example in [6, Section 5]. We show in Figure 4 the same numerical example as in Figure 2 but now overlaying the limiting one dimensional solution of the Laplace problem coupled with the coupling conditions (3) in red. We see that the 1D model gives a very good approximation already when the channels are quite wide, and the height converges when the channels become thinner proportional to the channel width.

The coupling conditions in Theorem 1 do not depend on the angles at the junction. If we go back to the channel flow problem in Figure 1 on the left, this does not seem to be a good approximation when the channels are still having a certain, albeit small width, since water will flow much more easily into a channel that goes along the flow direction, than into a channel that bifurcates in the opposite direction. In order to get more insight, we perform now a numerical experiment for the wave equation,

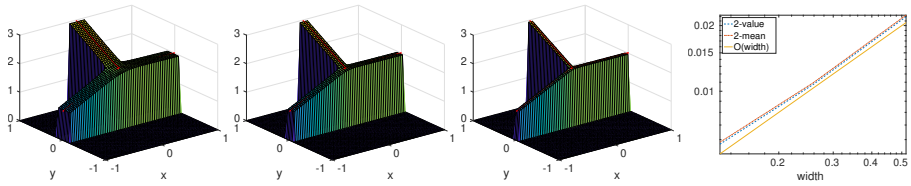

Fig. 4 Overlaid in red the limiting 1D Laplace problem with appropriate coupling conditions at the junction. Right: convergence of the numerical volume model to the exact junction height of the 1D model of the center value and average of the coupling domain Ω_0.

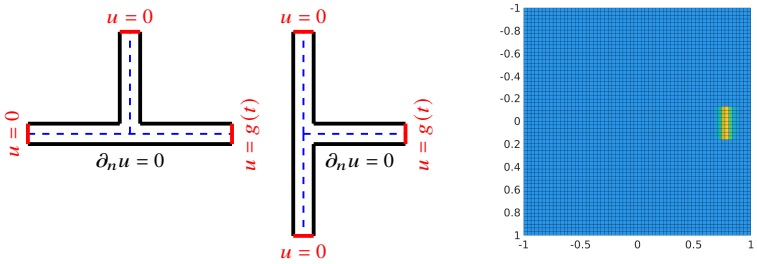

Fig. 5 Left and Middle: two T-shaped channel configurations for the wave equation experiment. Right: incoming planar Gaussian pulse seen from the top.

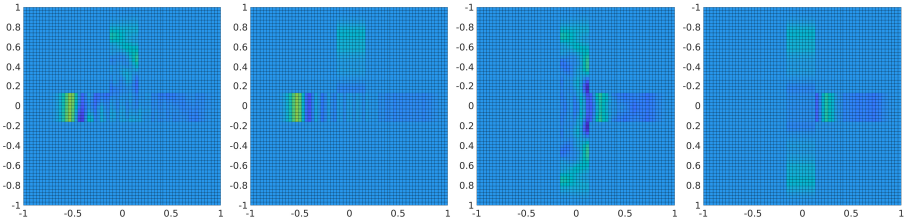

Fig. 6 From left to right: wave after passing the first T-shaped junction; corresponding averaged wave height across the channel width; wave after passing the second T-shaped junction; and corresponding averaged wave height across the channel width.

$$\partial_{tt} u = \Delta u \tag{4}$$

in two T-junction configurations as shown in Figure 5, with an incoming planar Gaussian pulse $u = g$ on the right and $\partial_n u = 0$ on lateral channel borders. We show in Figure 6 how the wave propagates through the two different channel configurations. We clearly see that the geometry of the junction plays a role: in the first case, most of the wave passes straight through the junction, and only a smaller part is deflected towards the top. This becomes especially visible if one plots average wave heights across the channel width, which would correspond to what a 1D model could deliver. In the second case, an equal part of the wave goes to the top and bottom channel, and a major part is reflected, again best visible in the averaged plot on the right. Clearly, for

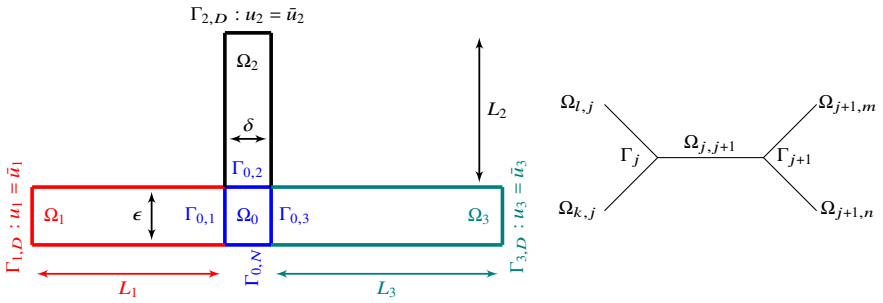

Fig. 7 Left: geometry for the Fourier analysis to solve the Laplace problem with zero Neumann boundary conditions on the channel sides. Right: notation for a small part of a very large network.

such problems a correction is needed for the geometry in the transmission conditions, the Kirchhoff type conditions of Theorem 1 in the limiting case are not good enough[1].

We therefore perform a Fourier Analysis for the Laplace problem $\Delta u = 0$ with zero Neumann boundary conditions on the channel sides of the specific geometry shown in Figure 7 (left). Cosine expansions of u_1 and u_3 in y and u_2 in x, together with a decomposition in the coupling domain $u_0 = v_0 + w_0$, where

$$\begin{cases} v_0 = 0 \text{ on } \Gamma_{0,1}, \Gamma_{0,3}, \\ \partial_y v_0 = 0 \text{ on } \Gamma_{0,N}, \\ \partial_y v_0 = \partial_y u_2 \text{ on } \Gamma_{0,2}, \end{cases} \quad \text{and} \quad \begin{cases} \partial_y w_0 = 0 \text{ on } \Gamma_{0,N}, \Gamma_{0,2}, \\ w_0 = u_1 \text{ on } \Gamma_{0,1}, \\ w_0 = u_3 \text{ on } \Gamma_{0,3}, \end{cases} \tag{5}$$

and a sine expansion of v_0 in x and a cosine expansion of w_0 in y lead to the exact solution in the T channel given in form of infinite series, and one can obtain a first theoretical result from these expansions:

Theorem 2 *The zeroth order term in the expansion leads again to the Kirchhoff coupling conditions from Theorem 1.*

Proof. It suffices to consider the zero order modes of the 6 coupling conditions

$$u_j = u_0 \quad \text{and} \quad \partial_n u_j = \partial_n u_0 \quad \text{on} \quad \Gamma_{0,j}, \quad j = 1, 2, 3.$$

Focusing on the 4 equations that are necessary at order 0, we solve the Laplace problem $\Delta u = 0$ on each subdomain, using on the domain Ω_0 the boundary conditions

$$w_0 = u_1 (:= \bar{u}_{01}) \text{ on } \Gamma_{0,1}, \quad w_0 = u_3 (:= \bar{u}_{03}) \text{ on } \Gamma_{0,3}, \quad \partial_y v_0 = \partial_y u_2 \text{ on } \Gamma_{0,2},$$

and on domain Ω_2, $u_2 = u_0 (:= \bar{u}_{20})$ on $\Gamma_{0,2}$. Now we expand the traces $\bar{u}_{01}$, $\bar{u}_{03}$ and $\bar{u}_{20}$ on the boundaries into a cosine series, and the trace $\partial_y u_2$ into a sine series. After some computations, we obtain at order 0 the equation

[1] If one makes the channels smaller (not shown here), the two junctions start to behave more and more the same, so in the limit, the Kirchhof law is still correct!

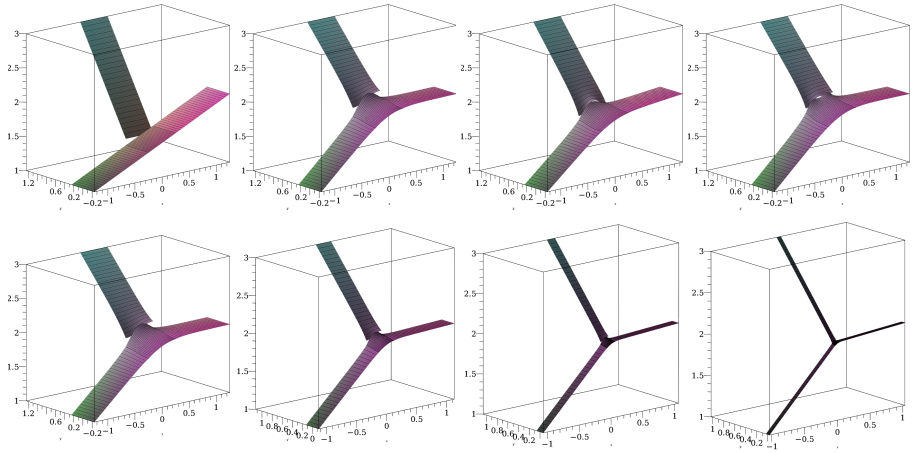

Fig. 8 Results for the Fourier approximation for the same channel configuration as in Figure 2 for the finite difference method. Top row: for $\delta = \epsilon = \frac{1}{2}$ with 1, 2, 3 and 4 Fourier modes. Bottom row: with 2 Fourier modes, from left to right with $\delta = \epsilon = \frac{1}{2}, \frac{1}{4}, \frac{1}{8}, \frac{1}{16}$.

	$\epsilon = \delta = \frac{1}{2}$	$\epsilon = \delta = \frac{1}{4}$	$\epsilon = \delta = \frac{1}{8}$	$\epsilon = \delta = \frac{1}{16}$
1 mode	1.500000000	1.500000000	1.500000000	1.500000000
2 modes	1.933582692	1.933116406	1.932865198	1.932734661
3 modes	1.858703806	1.855656687	1.854035147	1.853198023
4 modes	1.943070069	1.946462675	1.948287673	1.949235226

Table 1 Height of the middle point in the coupling domain Ω_0 in the Fourier approximation.

$$\frac{\bar{u}_{01,0} - \bar{u}_{1,0}}{L_1} + \frac{\delta}{\epsilon}\frac{\bar{u}_{20,0} - \bar{u}_{2,0}}{L_2} + \frac{\bar{u}_{03,0} - \bar{u}_{3,0}}{L_3} = 0,$$

where $\bar{u}_1, \bar{u}_2, \bar{u}_3$ are defined in Fig. 7 (left) and $\bar{u}_{x,0}$ is the zeroth mode of $\bar{u}_x$. □

We show in the top row of Figure 8 the coupled analytical solution from Theorem 2 using 1, 2, 3 and 4 Fourier modes in the expansion, for the same T-junction channel configuration as in Figure 2, and in the bottom row the approximation with 2 Fourier modes when the channel width decreases. We visually see that the Fourier approximation converges when more Fourier modes are added, and also that the coupled solution converges to the Kirchhoff limit when the channel becomes finer. To get more quantitative information, we show in Table 1 the numerical value of the center point in the junction domain Ω_0. We see that with only the constant mode, the height is not well approximated, even though according to Theorem 2, the correct asymptotic coupling conditions are used; see also Figure 8 at the top left. Adding more terms in the Fourier expansion corrects this rapidly, but we also see that convergence is not monotonic: with 3 modes the center height is lower than with 2 or 4 modes. We also see that when the channel width becomes smaller, the approximate heights converge to a limit, but the low number of modes does not yet suffice to see how convergence to the limiting height 2 occurs when the channel width goes

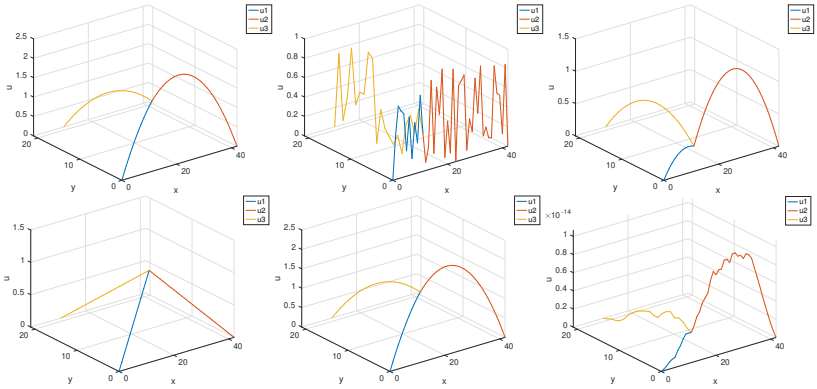

Fig. 9 Top row: solution, random initial guess u^0 and solution u^1 after subdomain solves with Lions' parallel Schwarz method without overlap. Bottom row: error $u - u^1$ after subdomain solves, solution after the coarse correction, and error after the coarse correction.

to zero, in contrast to what we observed in the finite difference approximation. This indicates that it will not be easy to obtain a theoretical convergence rate from this Fourier expansion.

3 Two Level Solver for the Laplace Problem

In order to solve a very large network in a scalable way, we propose now a specific two level method. We show the notation we use in Figure 7 (right). Brockmann proposes in [4] solving such problems on metric graphs using multigrid methods. To solve $\Delta u = f$ on such a graph is however one of the few examples where a 2-level DD method can become a direct solver, i.e. there exists a practical, truly optimal coarse space, which does not just provide scalability, and we have the following

Theorem 3 *Starting from an arbitrary initial guess u^0 on the network and applying one iteration of Lions' parallel Schwarz method with subdomains $\Omega_{j,j+1}$ without overlap (!),*

$$\Delta u^1_{j,j+1} = f \text{ in } \Omega_{j,j+1}, \quad u^1_{j,j+1} = u^0 \text{ on } \Gamma_j \text{ and } \Gamma_{j+1}, \tag{6}$$

the method gives the exact solution if next a coarse correction is applied with a piecewise linear coarse space aligned with $\Omega_{j,j+1}$.

We illustrate this result in Figure 9 for a T-channel network example with source term $f = 1$ and zero Dirichlet boundary conditions at the channel ends. Note that the Schwarz method without overlap does not converge, it only provides the influence of the right hand side from each subdomain here in the first iteration. The coarse correction then provides precisely the necessary piecewise linear complement so that the sum forms the solution on the network.

4 Conclusions

We used the Laplace problem on a graph to derive classical Kirchhoff type coupling conditions at junctions for a lower dimensional model. We showed numerically that these conditions give good approximations for the Laplace problem, but not for a wave propagation problem, since in the Kirchhoff type coupling conditions the angle dependence is lost. We then derived, again for the Laplace operator, an exact Fourier representation of the solution in the specific geometric configuration of a T junction. The first Fourier mode leads again to the Kirchhoff type coupling conditions. We also studied numerically the influence of the higher order Fourier modes. We finally showed that a non-overlapping two level Schwarz method can become a direct solver on such channel network models.

References

1. Bellamoli, F., Müller, L.O., Toro, E.F.: A numerical method for junctions in networks of shallow-water channels. Applied Mathematics and Computation **337**, 190–213 (2018)
2. Bressan, A., Canic, S., Garavello, M., Herty, M., Piccoli, B.: Flows on networks: recent results and perspectives. EMS Surv. Math. Sci. **1**(1), 47–111 (2014). DOI 10.4171/EMSS/2. URL https://doi.org/10.4171/EMSS/2
3. Briani, M., Puppo, G., Ribot, M.: Angle dependence in coupling conditions for shallow water equations at channel junctions. Computers & Mathematics with Applications **108**, 49–65 (2022)
4. Brockmann, M.: Multigrid method based on finite elements on metric graphs. Chemnitz FE Symposium 2023 (2023)
5. Caputo, J., Dutykh, D., Gleyse, B.: Coupling conditions for water waves at forks. Symmetry **11**(3), 434 (2019). DOI 10.3390/sym11030434. URL https://doi.org/10.3390/sym11030434
6. Exner, P., Post, O.: Convergence of spectra of graph-like thin manifolds. Journal of Geometry and Physics **54**(1), 77–115 (2005)
7. Garavello, M.: A review of conservation laws on networks. Networks & Heterogeneous Media **5**(3), 565 (2010)
8. Gugat, M., Leugering, G., Schittkowski, K., Schmidt, E.G.: Modelling, stabilization, and control of flow in networks of open channels. Online optimization of large scale systems pp. 251–270 (2001)
9. Holden, H., Risebro, N.H.: Riemann problems with a kink. SIAM journal on mathematical analysis **30**(3), 497–515 (1999)
10. Lagnese, J., Leugering, G., Schmidt, E.G.: Spectral analysis and numerical simulation of 1-d networks. Modeling, Analysis and Control of Dynamic Elastic Multi-Link Structures pp. 135–199 (1994)
11. Mehra, M., Shukla, A., Leugering, G.: An adaptive spectral graph wavelet method for PDEs on networks. Advances in Computational Mathematics **47**, 1–29 (2021)
12. Quarteroni, A., Formaggia, L.: Mathematical modelling and numerical simulation of the cardiovascular system. Handbook of numerical analysis **12**, 3–127 (2004)
13. Quarteroni, A., Ragni, S., Veneziani, A.: Coupling between lumped and distributed models for blood flow problems. Computing and Visualization in Science **4**(2), 111–124 (2001)
14. Van Thang, P., Chopard, B., Lefèvre, L., Ondo, D.A., Mendes, E.: Study of the 1D lattice Boltzmann shallow water equation and its coupling to build a canal network. Journal of Computational Physics **229**(19), 7373–7400 (2010)